Journal of Alloys and Compounds 508 (2010) 610–615

Contents lists available at ScienceDirect

Journal of Alloys and Compounds

journal homepage: www.elsevier.com/locate/jallcom

Low-temperature synthesis and characterization of complex perovskite $(Ca_{0.61}, Nd_{0.26})TiO_3$–$(Nd_{0.55}, Li_{0.35})TiO_3$ nanopowders and ceramics by sol–gel method

Qi-Long Zhang, Fei Wu, Hui Yang*, Jin-Feng Li

Department of Materials Science and Engineering, Zhejiang University, Hangzhou 310027, China

ARTICLE INFO

Article history:
Received 25 March 2010
Received in revised form 26 August 2010
Accepted 27 August 2010
Available online 6 September 2010

Keywords:
Sol–gel processes
Nanocomposites
Dielectric properties
Perovskites
Substrates

ABSTRACT

A sol–gel process was adopted to synthesize nanopowder with composition of $(1-x)(Ca_{0.61}, Nd_{0.26})TiO_3$–$x(Nd_{0.55}, Li_{0.35})TiO_3$ which was used to prepare the dielectric ceramics. As $x \leq 0.8$, pure solid solution phase with $GdFeO_3$-type perovskite structure could be obtained by calcining the xerogels at 500 °C. At $x = 0.6$, the particle size calculated from the transmission electron micrograph of powder was in the range of 30–50 nm. Ceramics prepared by the nanoparticles at 1150 °C exhibited good dielectric properties with dielectric constant (ε_r) of 93.4, a $Q \times f$ value of 7115 GHz and τ_f value of 0 ppm/°C, which have great improvement in $Q \times f$ value and decreased the sintering temperature compared with the ceramics synthesized by solid-state method. HRTEM images showed superstructure, indicating that the solid solution phase with ordering crystal structure is helpful to the dielectric properties improvement.

1. Introduction

Dielectric ceramics appropriate for microwave application as resonators and filters are required to have moderate relative permittivity (ε_r), low dielectric loss–high-quality factor (Q) at a resonant frequency (f) in gigahertz range as well as a near-zero temperature frequency coefficient (τ_f) [1]. High-permittivity ceramics are necessary for the miniaturization of passive microwave components. $(Ca_{1-x}, Nd_{2x/3})TiO_3$ has been viewed as a potential candidate material for microwave dielectric applications because of its high dielectric constant [2–6]. The composition $x = 0.39$ revealed the highest $Q \times f$ value of 17,200 GHz and a high permittivity of 108 among all samples [2]. However, $(Ca_{1-x}, Nd_{2x/3})TiO_3$ ceramics also possessed a large positive τ_f value, which precludes their usage in practice. Targeting at compensating their τ_f values, an effective method has been developed to combine two or more compounds with negative and positive temperature coefficients, respectively, to form solid solutions or mixed phases [7–12], such as $ZnAl_2O_4$–TiO_2, (Ca, Mg)SiO_3–$CaTiO_3$, (Ca, Sm)TiO_3–TiO_3, $La(Mg_{1/2}Ti_{1/2})O_3$–$(Na_{1/2}Nd_{1/2})TiO_3$, TiO_2–$NiNb_2O_6$, and Zn_2TiO_4–TiO_2 complex ceramics. Results exhibited that zero τ_f values could be obtained at the proper composition ratio between the end members. In order to adjust τ_f values of the (Ca, Nd)TiO_3 ceramics, negative τ_f value ceramics (Li, Nd)TiO_3 as compensators were introduced to form (Ca, Nd)TiO_3–(Li, Nd)TiO_3 complex ceramics, which showed near-zero τ_f values. However, the $Q \times f$ value was decreased to 5300 GHz [6].

(Ca, Nd)TiO_3 and (Ca, Nd)TiO_3–(Li, Nd)TiO_3 complex ceramics were usually made by the solid-state reactions at high temperature (higher than 1350 °C) [13]. Under such high sintering temperature, grain growth and the volatilization of Li^+ which degraded the dielectric properties would happen. In contrast, wet-chemistry methods start with a homogeneous liquid solution of cation ingredients, with metal cations mixed in stoichiometric ratios at the atomic scale [14,15]. Therefore, pure samples at the nanometer scale could theoretically be obtained at lower temperatures and shorter reaction times than that afforded by solid-state reactions. In our previous study, ultrafine $(Ca_{0.61}, Nd_{0.26})TiO_3$ powder with 5–10 nm was synthesized by sol–gel method. Dense ceramics with good microwave dielectric properties could be achieved at low sintering temperature of 1200 °C using the synthesized powder [16]. It indicates that the sol–gel process is an effective route to prepare high-quality microwave ceramics.

In this paper, in order to improve the sintering characteristic and dielectric properties of (Ca, Nd)TiO_3–(Li, Nd)TiO_3 complex ceramics, we reported the $(1-x)(Ca_{0.61}, Nd_{0.26})TiO_3$–$xNd_{0.55}Li_{0.35}TiO_3$($(1-x)$CNT–$x$NLT) nanopowders synthesized by sol–gel process. Sintering behavior and dielectric properties of CNT–NLT ceramics prepared by nanopowders were studied.

2. Experimental procedures

Neodymium nitrate tetrahydrate ($Nd(NO_3)_3{\cdot}6H_2O$, Aldrich, 99.9%), lithium nitrate ($LiNO_3$, Aldrich, 99.9%), tetrabutyl titanium ($Ti(C_4H_9O)_4$, Aldrich, 98%), and

* Corresponding author. Tel.: +86 571 87951408; fax: +86 571 87951408.
E-mail address: mse237@zju.edu.cn (H. Yang).

0925-8388/$ – see front matter © 2010 Elsevier B.V. All rights reserved.
doi:10.1016/j.jallcom.2010.08.140

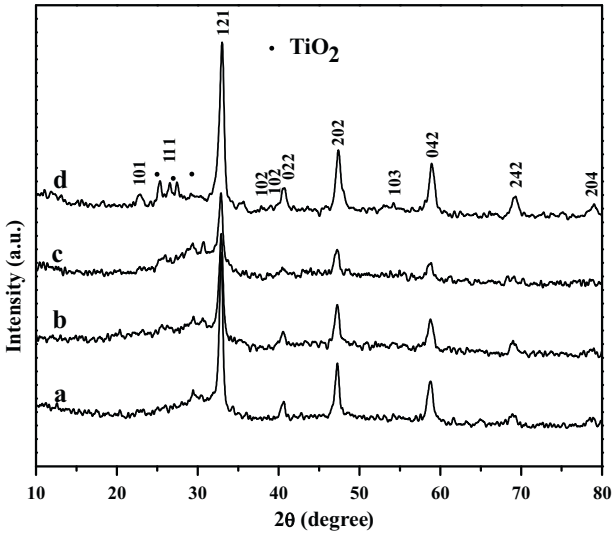

Fig. 1. XRD patterns of $(1-x)(Ca_{0.61}, Nd_{0.26})TiO_3$–$x(Nd_{0.55}, Li_{0.35})TiO_3$ xerogels calcined at 500 °C for 1 h: (a) $x = 0.2$, (b) $x = 0.4$, (c) $x = 0.6$, (d) $x = 0.8$.

calcium nitrate tetrahydrate ($Ca(NO_3)_2{\cdot}4H_2O$, 99.9%) were used as the starting materials. Nitric acid was employed to adjust the pH value. The PEG400 was used as surfactant and absolute ethanol was used as the reaction media for the dispersion of $(1-x)$CNT–xNLT nanoparticles.

Sol–gel synthesis method of the $(Ca_{0.61}, Nd_{0.26})TiO_3$ nanoparticles was described in detail elsewhere [16]. $(Nd_{0.55}, Li_{0.35})TiO_3$ sol was prepared by the following process. 34.02 g of $Ti(C_4H_9O)_4$ was added to 100 ml ethanol with continuous stirring using a magnetic stirrer for 1 h. 21.3 g of $Nd(NO_3)_3{\cdot}6H_2O$ and 2.52 g of $LiNO_3$ were dissolved into 55 ml and 35 ml ethanol solution, respectively, and then were dropped into the $Ti(C_4H_9O)_4$ ethanol solution. Nitric acid was used to adjust the $H^+/Ti^{4+} = 0.4385$ and PEG400 with 4 wt% was employed as surfactant. After continuous stirring for 2 h, the sol was aged for 24 h and then 14.4 g deionized water was added to the sol with vigorous stirring for 1 h. $(Ca_{0.61}, Nd_{0.26})TiO_3$ nanoparticles were added to the $(Nd_{0.55}, Li_{0.35})TiO_3$ sol according to x value ($x = 0.2$, 0.4, 0.6, 0.8), and the sol with CNT nanoparticles was stirred until they turned into gel completely and then the gel was aged for 48 h. The wet gel was dried and then calcined at 500 °C for 1 h to form the CNT–NLT nanoparticles. The obtained compound nanoparticles were ball-milled in ethanol medium for 2 h by planner-milling and then dried. For the sintering experiments, the dried nanopowders were mixed with 6% PVA solution and subsequently uniaxially pressed into cylindrical pellets of 18 mm diameter and 9 mm thickness under a pressure of 30 MPa. Conventional sintering was performed at 25 °C temperature intervals between 1100 to 1200 °C for 2 h.

Crystal phases of the nanoparticles and ceramics were investigated by X-ray powder diffraction (XRD) analysis using Cu-Kα radiation from 10° to 80° with a step size of 0.02° and a count time of 2 s. Scanning electron microscope (SEM, JEM-480) was used to characterize the microstructure of the ceramics. Transmission electron microscopy (TEM) was performed with a JEOL-J2010 operated at 200 kV. Samples were prepared by grinding the as-synthesized ceramics, suspending in a chloroform solution grid. HRTEM images and selected area electron diffraction (SAED) patterns were taken. Microwave dielectric constant (ε_r) and quality factor value at microwave frequency ($Q \times f$) were measured using Hakki–Coleman method and cavity method by vector network analysis (Agilent 8719ET, USA), respectively. The temperature coefficient of resonant frequency (τ_f) was measured in temperature ranging from 25 to 80 °C at microwave frequency.

3. Results and discussion

XRD patterns of the as-prepared $(1-x)$CNT–xNLT gel with different x values calcined at 500 °C for 1 h are shown in Fig. 1. $GdFeO_3$-type solid solution phase as major phase along with several small peaks attributed to rutile TiO_2, was observed in the composition range. $GdFeO_3$-type solid solution phase has no obvious change but TiO_2 phase increases gradually with increasing x value. Fig. 2 shows the TEM image of $(1-x)$CNT–xNLT powder obtained by calcining the xerogels with $x = 0.6$ at 500 °C for 1 h. The particle size calculated from the TEM was in the range of 30–50 nm.

Fig. 3 illustrates ceramic samples prepared by the nanopowders with different x values sintered at 1150 °C for 2 h. As expected, CNT and NLT formed $GdFeO_3$-type perovskite structure solid solution. Pure $GdFeO_3$-type solid solution phase is obtained with the x value less than 0.6. At $x = 0.8$, the rutile TiO_2 appears, and the (2 0 2), (0 4 2), (2 4 2), (2 0 4) diffraction peaks of $GdFeO_3$-type solid-state phase displace to a higher 2θ angle indicating the decrease in the unit cell volume. Fig. 4 shows the SEM photographs of surfaces of $(1-x)$CNT–xNLT samples sintered at 1150 °C for 2 h. The samples with different x values have dense microstructure and the size of the grains is about 0.5–2 μm. SEM images of surfaces of the samples with $x = 0.6$ at different sintering temperatures are shown in Fig. 5. Specimens sintered at 1100 °C are not completely dense and a small amount of porosity can be observed, the grain size is about 1–2 μm. Well-sintered dense ceramics are obtained for samples sintered at temperatures between 1125 and 1175 °C. The increase of sintering temperature leads to promote the grain growth and a relative increase in the grain size can be achieved. However, over high sintering temperature causes the abnormal grain growth. As shown in Fig. 5(d), samples sintered at 1175 °C have the severe abnormal grain growth, and parts of the abnormal elongated grain size is larger than 5 μm. This experiment shows that, the sintering temperature of the well-sintered ceramics synthesized by sol–gel process is much lower than that of the solid-reaction method [13]. The result indicated that the nanoparticles with high ratio of specific surface area and surface energy contributed to promote sintering properties and reduce sintering temperature.

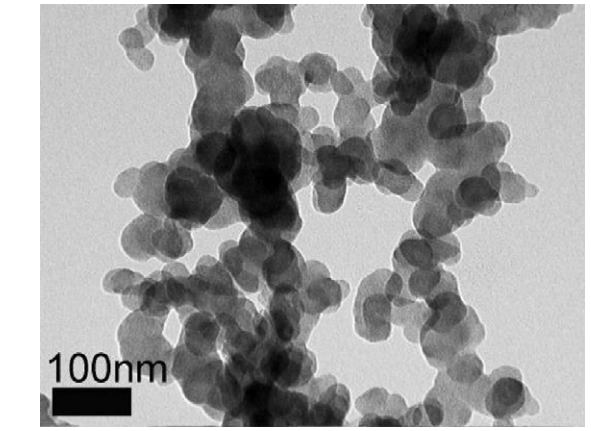

Fig. 2. TEM image of $(1-x)(Ca_{0.61}, Nd_{0.26})TiO_3$–$x(Nd_{0.55}, Li_{0.35})TiO_3$ with $x = 0.6$ xerogels calcined at 500 °C for 1 h.

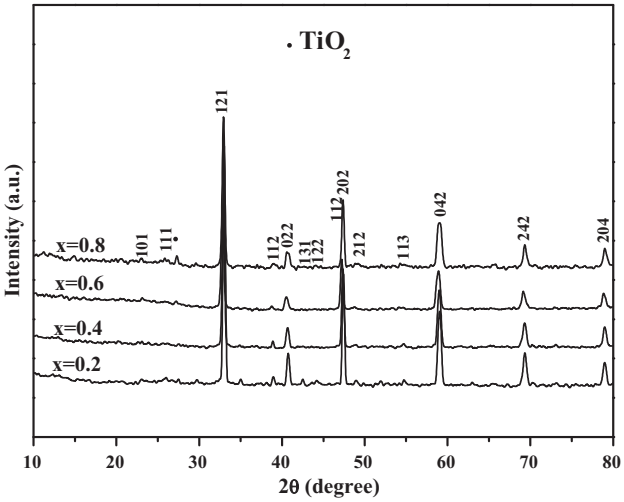

Fig. 3. XRD patterns of $(1-x)(Ca_{0.61}, Nd_{0.26})TiO_3$–$x(Nd_{0.55}, Li_{0.35})TiO_3$ ceramics sintered at 1150 °C for 2 h.

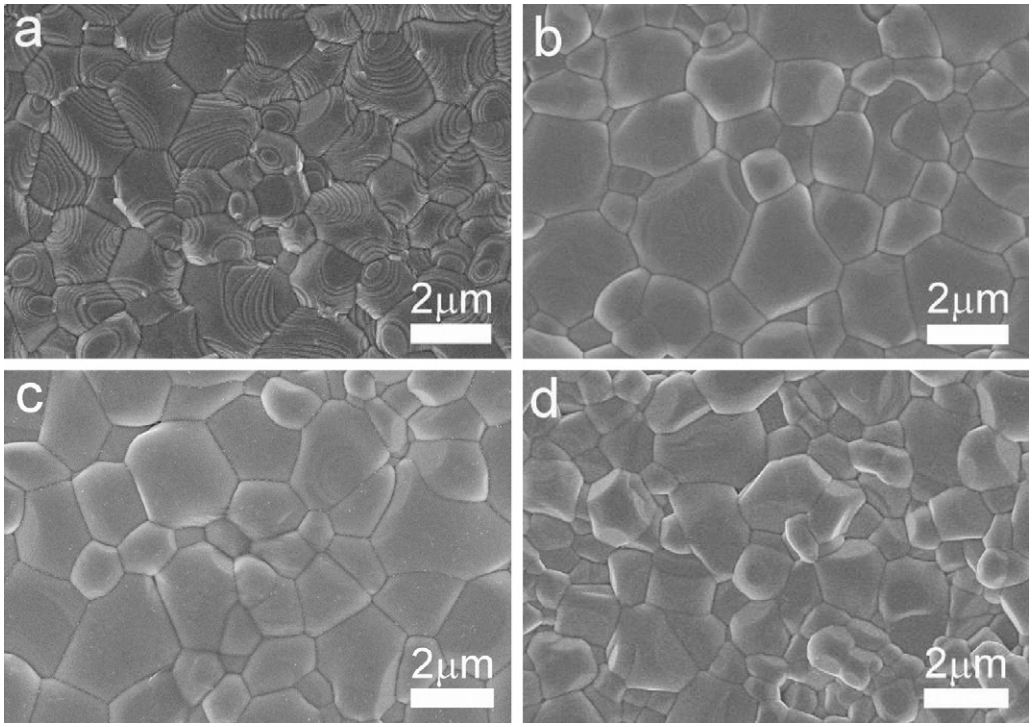

Fig. 4. SEM images of $(1-x)(Ca_{0.61}, Nd_{0.26})TiO_3$–$x(Nd_{0.55}, Li_{0.35})TiO_3$ sintered at 1150 °C for 2 h: (a) 0.2, (b) 0.4, (c) 0.6, (d) 0.8.

Table 1 shows the dielectric properties of $(1-x)$CNT–xNLT samples. At 1200 °C, very dense CNT ceramics with uniform grains [16] and good dielectric properties with a dielectric constant (ε_r) of 90.2, a quality factor ($Q \times f$) of 25,200 GHz, and a temperature coefficient of resonant frequency (τ_f) of 243 ppm/°C were achieved. However, NLT ceramics sintered at 1150 °C have very large negative τ_f value of −77 ppm/°C with a lower permittivity of 86.52 and $Q \times f$ value of 8256 GHz. With the x value increasing from 0.2 to 0.8, the $Q \times f$ value decreases rapidly, the dielectric constant (ε_r) increases firstly and obtains the maximum of 96.3 at $x = 0.4$ and then decreases. The τ_f value, as expected, changed from 129 to −74.1 ppm/° as x increased from 0.2 to 0.8. The phase constitute including second phase is a more important factor than porosity to affect the dielectric properties of microwave ceramics having over 90% of relative density [17]. It can be seen that all samples shown in Fig. 4 show a very dense structure. Thus, the dielectric properties are mainly depen-

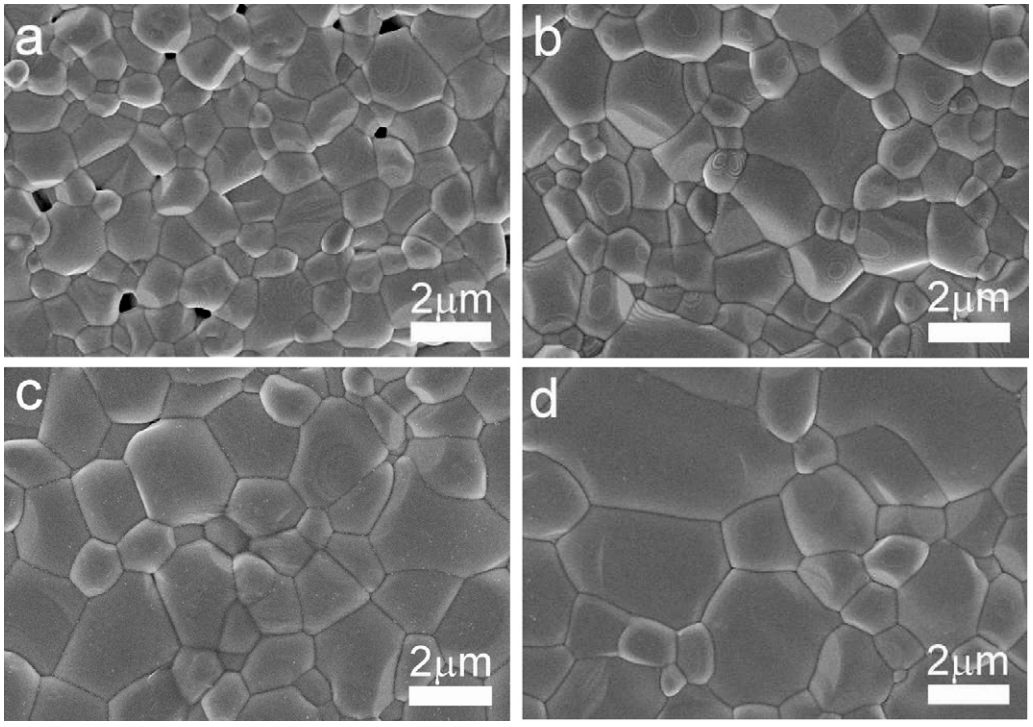

Fig. 5. SEM images of $(1-x)(Ca_{0.61}, Nd_{0.26})TiO_3$–$x(Nd_{0.55}, Li_{0.35})TiO_3$ with $x = 0.6$ sintered at (a) 1100 °C, (b) 1125 °C, (c) 1150 °C, (d) 1175 °C.

Table 1
Dielectric properties of $(1-x)(Ca_{0.61}, Nd_{0.26})TiO_3$–$x(Nd_{0.55}, Li_{0.35})TiO_3$ ceramics.

x value	$Q \times f$ (GHz)	ε_r	τ_f (ppm/°C)	Sintering temperature (°C)
0	25,200	90.2	243	1200
0.2	11,045.2	90.0	129	1150
0.4	9418	96.3	32.04	1150
0.6	7114.5	93.4	0	1150
0.8	4590	86.8	−74.1	1150
1	8256	86.52	−77	1150

dent on the composition and the second phase. More NLT results in the decrease of the $Q \times f$ value, and the τ_f value shift to a negative value. However, the cause that the maximum ε_r can be achieved at $x = 0.4$ is still unclear. As shown in Fig. 3, the specimens of $x \geq 0.6$ have a small of TiO_2 with high permittivity ($\varepsilon_r = 100$) and a very large positive τ_f value ($\tau_f = 450$ ppm/°C) [18], which was helpful in increasing ε_r and τ_f. However, the content of NLT ceramics is much higher than that of TiO_2. As a whole, the NLT content is still the major factor causing the decrease of ε_r and τ_f.

Dielectric constant and $Q \times f$ value of samples with $x = 0.6$ for $(1-x)$CNT–xNLT ceramics sintered at different temperatures are shown in Fig. 6. The dielectric constant is only 86.0 at 1100 °C and obtains its maximum value of 99.59 at 1125 °C and then decreases to 93.4 at 1150 °C. However, further increasing the temperature leads to the increase in ε_r again. Well-sintered dense ceramics can

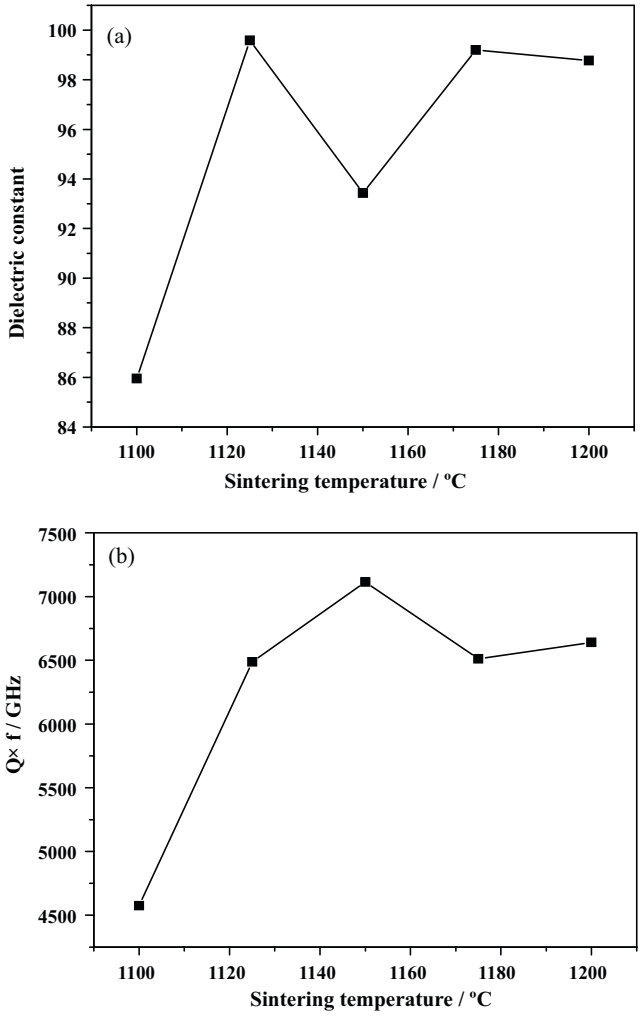

Fig. 6. Dielectric properties of $(1-x)(Ca_{0.61}, Nd_{0.26})TiO_3$–$x(Nd_{0.55}, Li_{0.35})TiO_3$ ceramics sintered at different temperatures with $x = 0.6$: (a) dielectric constant, (b) $Q \times f$ value.

be obtained at 1150 °C, as shown in Fig. 5(c). Unfortunately, the cause of the decrease in ε_r is unclear and would be further studied in our future work. The $Q \times f$ value increases firstly and then achieves the maximum of 7114.5 GHz at 1150 °C. Many factors could affect the dielectric properties such as lattice vibration modes, secondary phases, porosity, inhomogeneity and grain size [19,20]. Generally, a larger grain size and a smaller grain boundary indicate reduction in imperfection and dielectric loss. Samples sintered at 1100 °C with low ε_r and $Q \times f$ value are attributed to a low bulk density and small grains as shown in Fig. 5(a). As the sintering temperature increased from 1100 to 1150 °C, the $Q \times f$ value increased due to grain size augment and grain boundary reduction. After reaching a maximum at 1150 °C, inhomogeneous distribution of grain and abnormal growth lead to the decrease of the $Q \times f$ value. At 1150 °C, the high-quality CNT–NLT ceramic with a dielectric constant of 93.4, a $Q \times f$ value of 7114 GHz and a τ_f value of 0 ppm/°C for $x = 0.6$ was obtained.

Compared to the samples prepared by the conventional solid-reaction method, as reported in [2,21], samples prepared by nanopowders obtained by sol–gel route, have higher $Q \times f$ values. $(Nd_{0.55}, Li_{0.35})TiO_3$ ceramics is a kind of A-site ordering complex oxide with perovskite structure which have the same structure and space group pmna (62) with $(Ca_{0.61}, Nd_{0.26})TiO_3$ ceramics. A-site ordering in $(Nd_{2x/3}, Li_x)TiO_3$ system ceramics can improve the dielectric properties [22]. HRTEM and the corresponding SAED images taken along [0 0 1] and [1 1 0] direction are shown in Fig. 7 to get the further microstructure information of the ceramics. In the images of the sample parallel to [1 1 0] axis, the SAED pattern shows the presence of the $(\bar{1}\,0\,0)$ reflections. Besides, there are faint satellite reflections at $(h/2\ k/2\ 1)$, suggesting the existence of modulated structure along these directions which is caused by the defects demonstrated by the HRTEM image in Fig. 7(a) [23]. The lithium-containing compounds show a superstructure reflection along (0 0 1), most probably due to the ordering of occupied and empty A-sites along the alternate (0 0 1) plane [24]. Strong bright and faint spots ranged periodically along the two directions. It is observed that each bright spot or each faint spot has four faint spots or half bright and half faint spots around it and each square including 9 spots present along the [0 0 l] direction periodically, indicating that the solid solution consisted of $(Ca_{0.61}, Nd_{0.26})TiO_3$ and $(Nd_{0.5}, Li_{0.5})TiO_3$ phase unit cell does not distribute in the same direction and rotate along [0 0 1] axis for some degrees relatively. Therefore, the superlattice refraction of two kinds of perovskite structure phases along [0 0 1] direction in nanodomain is observed in Fig. 7(c). HRTEM image corresponding to the SAED pattern taken along [0 0 1] direction provides the further information that two kinds of patterns form the moiré pattern which demonstrates that although the two phases have the same perovskite structure and the space group, two different kinds of unit cells in the solid solution cannot match each other perfectly.

Taking into account the periodical bright and faint diffraction spots, we cannot observe the same overlapping pattern along the [1 1 0] axis, indicating that Ca^{2+}, Nd^{3+} ions and vacancies and Li^+, Nd^{3+} and vacancies form the alternating layer in A-site respectively and then octahedral tilting leads to the two alternating layers in

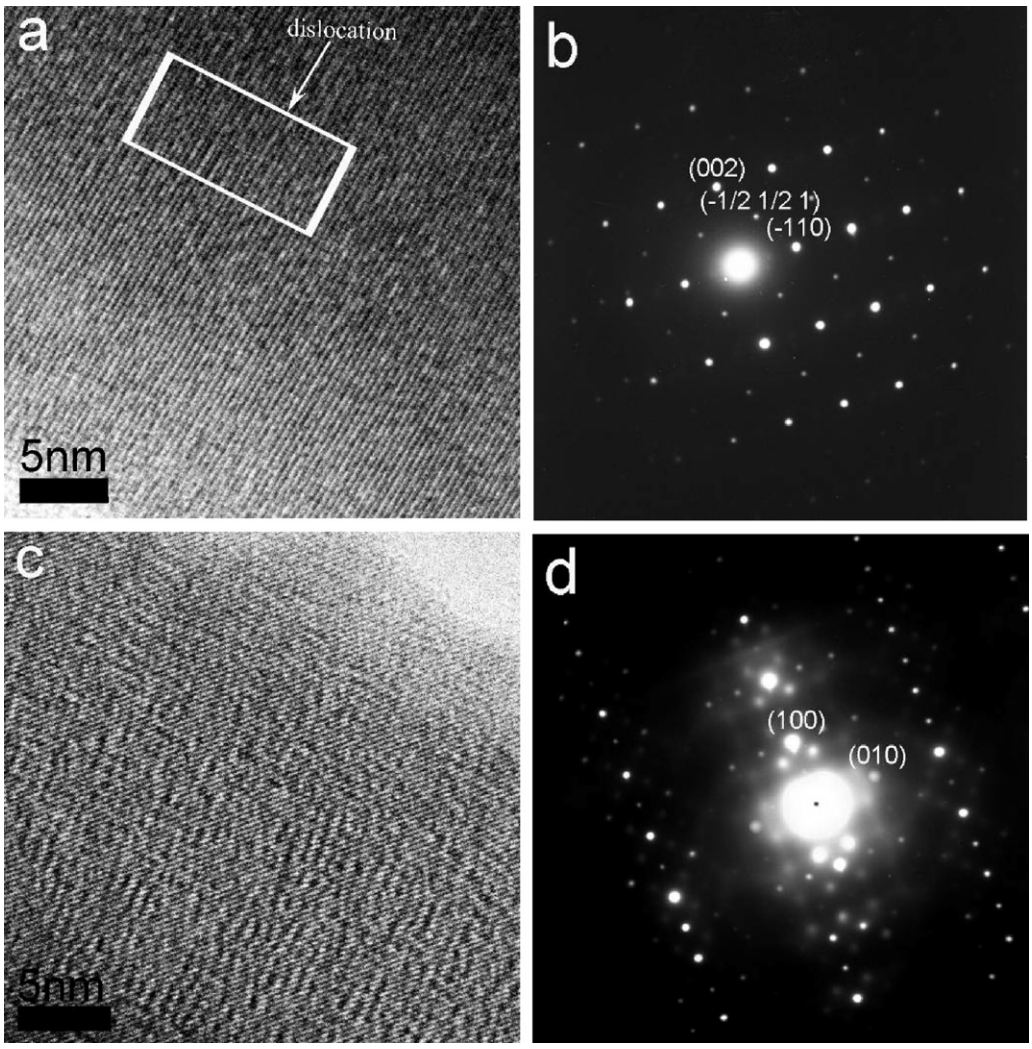

Fig. 7. High-resolution images and the corresponding selected area electron diffraction patterns of the particles of $(1-x)(Ca_{0.61}, Nd_{0.26})TiO_3$–$x(Nd_{0.55}, Li_{0.35})TiO_3$ ceramics with $x = 0.6$ sintered at 1150 °C for 2 h: (a) the HRTEM image taken with the electron beam parallel to [1 1 0], and (b) the corresponding SAED pattern, (c) the image taken with the electron beam parallel to [0 0 1], and (d) the corresponding SAED pattern.

different orientations. And both of the layers should keep their periodical permutation, which contributes the special solid solution structure. The vacancies and the octahedral tilting contribute to the extrinsic loss but not the secondary precipitation phase in the solid solution. Therefore, the solid solution phase with the ordering A-site layers in perovskite structure is helpful to the dielectric properties improvement.

4. Conclusions

Complex perovskite $(1-x)(Ca_{0.61}, Nd_{0.26})TiO_3$–$x(Nd_{0.55}, Li_{0.35})TiO_3$ nanopowders and ceramics are synthesized by sol–gel method. As $x \leq 0.8$, pure solid solution phase with $GdFeO_3$-type perovskite structure could be obtained by calcining the xerogels at 500 °C for 1 h. At $x = 0.6$, the particle size calculated by TEM was about 30–50 nm. Dense ceramics synthesized by the nanoparticles could be achieved at low-temperature of 1150 °C due to the effect of small size nanoparticles. Compared with conventional solid-state method, the sintering temperature is decreased about 150–200 °C. Sample of $x = 0.6$ sintered at 1150 °C exhibited good dielectric properties with dielectric constant (ε_r) of 93.4, a $Q \times f$ value of 7115 GHz and a τ_f value of 0 ppm/°C, which has higher $Q \times f$ value than the ceramics synthesized by solid-state method. HRTEM and SAED analyses have been taken to study the microstructure of the ceramics. The improvement of dielectric properties is attributed to the pure solid solution phase with the ordering perovskite crystal structure.

Acknowledgements

The authors thankfully acknowledge the financial support from National Key Technology Support Program (No. 2009BAG12A07).

References

[1] M.T. Sebastian, Dielectric Materials for Wireless Communication, first ed., Elsevier, Oxford, UK, 2008.
[2] M. Yoshida, N. Hara, T. Takada, A. Seki, Jpn. J. Appl. Phys. 36 (1997) 6818–6823.
[3] B.L. Liang, X.H. Zheng, D.P. Tang, J. Alloys Compd. 488 (2009) 409–413.
[4] M.S. Fu, X.Q. Liu, X.M. Chen, J. Eur. Ceram. Soc. 28 (2008) 585–590.
[5] C.H. Shen, C.L. Huang, C.F. Shih, C.M. Huang, J. Alloys Compd. 475 (2009) 391–395.
[6] H.L. Chen, C.L. Huang, Jpn. J. Appl. Phys. 41 (2002) 5650–5653.
[7] C.L. Huang, T.J. Yang, C.C. Huang, J. Am. Ceram. Soc. 92 (2009) 119–124.
[8] Q.L. Zhang, H. Yang, H.P. Sun, J. Eur. Ceram. Soc. 28 (2008) 605–609.
[9] T. Yamashita, J. Barry, R. Taylor, J. Am. Ceram. Soc. 93 (2010) 251–255.
[10] Y.B. Chen, J. Alloys Compd. 500 (2010) 190–194.
[11] Y.C. Liou, C.Y. Shiue, M.H. Weng, J. Eur. Ceram. Soc. 29 (2009) 1165–1171.
[12] C.F. Shih, W.M. Li, M.M. Lin, C.Y. Hsiao, K.T. Hung, J. Alloys Compd. 485 (2009) 408–412.
[13] Z. Yue, Y. Zhang, Z. Gui, L. Li, Appl. Phys. A 80 (2005) 1757–1761.

[14] J. Park, J. Joo, S.G. Kwon, Y. Jang, T. Hyeon, Angew. Chem. Int. Ed. 46 (2007) 4630–4660.
[15] U. Jeong, X. Teng, Y. Wang, H. Yang, Y. Xia, Adv. Mater. 19 (2007) 33–60.
[16] Q.L. Zhang, F. Wu, H. Yang, D. Zou, J. Mater. Chem. 18 (2008) 5339–5343.
[17] D.M. Iddles, A.J. Bell, A.J. Moulson, J. Mater. Sci. 27 (1992) 6303–6310.
[18] S.B. Cohn, IEEE Trans. Microwave Theor. Technol. MTT-16 (1968) 218–227.
[19] H.X. Yuan, X.Y. Chen, M.M. Mao, J. Am. Ceram. Soc. 99 (2009) 2286–2290.
[20] S.J. Penn, N.M. Alford, A. Tempeton, X.R. Wang, M.S. Xu, M. Reece, K. Schrapel, J. Am. Ceram. Soc. 80 (1997) 1885–1888.
[21] W.S. Kim, K.H. Yoon, E.S. Kim, Jpn. J. Appl. Phys. 39 (2000) 5650–55653.
[22] J.J. Bian, G.S. Song, K. Yan, Ceram. Int. 34 (2008) 893–896.
[23] S.G. Martin, F.G. Alavrado, A.D. Robertson, A.R. West, M.A. Alario-Franco, J. Solid State Chem. 128 (1997) 97–101.
[24] S.G. Martin, M.A. Alario-Franco, J. Solid State Chem. 148 (1999) 93–99.